Table 1. $A\beta_{40}$ and $A\beta_{42}$ levels in wild-type and neprilysin-deficient mice. $A\beta_{40}$ and $A\beta_{42(43)}$ were extracted from mouse brains by guanidine hydrochloride and quantified as described (*6*). The antibodies for the ELISA were generously provided by Takeda Chemical Industries, Ltd. Eight-week-old male mice were used for all experiments. We performed eight independent measurements to examine the effect of neprilysin deficiency using more than 50 mice; all the results were consistent. For neprilysin, $n = 9$ mouse brains; for presenilin, $n = 3$ mouse brains. The amounts of APP and its proteolytic fragments remained unchanged in neprilysin$^{-/-}$ mice as analyzed by Western blotting (*30*). The positive control data were taken in an identical manner using mutant presenilin-1 knock-in mice (*18*). Each value represents the average ± SE with the indicated number of animals.

Genotype	$A\beta_{40}$ (pmol/g)	$A\beta_{42}$ (pmol/g)
	Neprilysin	
+/+ (control littermates)	1.084 ± 0.075	0.253 ± 0.011
+/−	1.475 ± 0.047*	0.398 ± 0.045*
−/−	2.174 ± 0.130*	0.541 ± 0.063*
	Mutant presenilin 1	
−/− (control littermates)	1.047 ± 0.138	0.252 ± 0.036
−/+	1.176 ± 0.183	0.368 ± 0.029†

*$P < 0.001$ and †$P < 0.01$, as compared to control littermates by Student's *t* test.

script containing exon 1, whereas the other forms are the major transcripts found in other tissues, the enhancer and promoter regions upstream of exon 1 (*23–25*) are likely to selectively regulate the total expression level of neprilysin in neurons. Indeed, there are several clusters of possible transcription factor (TF) binding sites, at least one identified enhancer, and two dinucleotide repeats in the upstream region (Fig. 3B). Removal of the enhancer sequence leads to more than 90% reduction in promoter activity (*25*). The neprilysin gene also possesses two androgen-responsive elements (*26*), which might be associated with the lower incidence of the disease among males than females (*27*). Therefore, it may be possible that some of the mutations or polymorphisms in these and related regions could influence the expression of neprilysin in a neuron-specific manner and consequently alter Aβ levels in the brain. Such mutations or polymorphisms can be either a risk factor or protective factor, depending on whether they cause down- or up-regulation of neprilysin expression. Although this assumption is a hypothetical prediction, the neprilysin gene is indeed located within the candidate chromosome 3 locus associated with late-onset AD cases (*28*, *29*) and is, therefore, a potential target in the search for genetic risk factors.

References and Notes

1. J. Hardy, *Trends Neurosci.* **20**, 154 (1997).
2. D. J. Selkoe, *Trends Cell Biol.* **8**, 447 (1998).
3. _____, *Trends Neurosci.* **16**, 403 (1993).
4. T. C. Saido, *Neurobiol. Aging* **19**, S69 (1998).
5. _____, *Neurosci. News* **5(3)**, 52 (2000).
6. N. Iwata *et al.*, *Nature Med.* **6**, 143 (2000).
7. K. Ikeda *et al.*, *J. Biol. Chem.* **274**, 32469 (1999).
8. S. Kiryu-Seo *et al.*, *Proc. Natl. Acad. Sci. U.S.A.* **97**, 4345 (2000).
9. K. Shirotani *et al.*, *J. Biol. Chem.*, in press (available at www.jbc.org/cgi/reprint/M008511200v1).
10. Y. Takaki *et al.*, *J. Biochem.* **128**, 897 (2000).
11. B. Lu *et al.*, *J. Exp. Med.* **181**, 2271 (1995).
12. K. Vekrellis *et al.*, *J. Neurosci.* **20**, 1657 (2000).
13. A. Perez, L. Morelli , J. C. Cresto, E. M. Castano, *Neurochem. Res.* **25**, 247 (2000).
14. H. M. Tucker *et al.*, *J. Neurosci.* **20**, 3937 (2000).
15. K. Duff *et al.*, *Nature* **383**, 710 (1996).
16. D. R. Borchelt *et al.*, *Neuron* **17**, 1005 (1996).
17. N. Sawamura *et al.*, *J. Biol. Chem.* **275**, 27901 (2000).
18. Y. Nakano *et al.*, *Eur. J. Neurosci.* **11**, 2577 (1999).
19. A. Saria *et al.*, *Neurosci. Lett.* **234**, 27 (1997).
20. K. Yasojima, H. Akiyama, E. G. McGeer, P. L. McGeer, *Neurosci. Lett.* **297**, 97 (2001).
21. H. Braak, E. Braak, *Acta Neuropathol.* **82**, 239 (1991).
22. T. Iwatsubo *et al.*, *Neuron* **13**, 45 (1994).
23. C. Li, R. M. Booze, L. B. Hersh, *J. Biol. Chem.* **270**, 5723 (1995).
24. H. Haouas *et al.*, *Biochem. Biophys. Res. Commun.* **207**, 933 (1995).
25. C. Li, L. B. Hersh, *Arch. Biochem. Biophys.* **358**, 189 (1998).
26. R. Shen *et al.*, *Mol. Cell. Endocrinol.* **170**, 131 (2000).
27. L. Fratiglioni *et al.*, *Neurology* **48**, 132 (1997).
28. R. E. Tanzi *et al.*, *Neurobiol. Dis.* **3**, 159 (1996).
29. S. E. Poduslo *et al.*, *Hum. Genet.* **105**, 32 (1999).
30. N. Iwata *et al.*, data not shown.

31. We thank T. Kudo and M. Takeda for providing mutant I213T presenilin 1 knock-in mice. We also thank T. Yoshikawa for valuable discussions; J. Q. Trojanowski, V. M.-Y. Lee, and T. Hensch for critical reading of the manuscript; and Y. Dohzono, M. Sekiguchi, E. Hosoki, and K. Watanabe for technical assistance. Funded by research grants from RIKEN BSI, Ministry of Education, Special Coordination Funds for promoting Science and Technology of STA, Ministry of Health and Welfare, and Takeda Chemical Industries.

16 February 2001; accepted 17 April 2001

Impairment of the Ubiquitin-Proteasome System by Protein Aggregation

Neil F. Bence, Roopal M. Sampat, Ron R. Kopito*

Intracellular deposition of aggregated and ubiquitylated proteins is a prominent cytopathological feature of most neurodegenerative disorders. Whether protein aggregates themselves are pathogenic or are the consequence of an underlying molecular lesion is unclear. Here, we report that protein aggregation directly impaired the function of the ubiquitin-proteasome system. Transient expression of two unrelated aggregation-prone proteins, a huntingtin fragment containing a pathogenic polyglutamine repeat and a folding mutant of cystic fibrosis transmembrane conductance regulator, caused nearly complete inhibition of the ubiquitin-proteasome system. Because of the central role of ubiquitin-dependent proteolysis in regulating fundamental cellular events such as cell division and apoptosis, our data suggest a potential mechanism linking protein aggregation to cellular disregulation and cell death.

The ubiquitin-proteasome system (UPS) functions in cellular quality control by degrading misfolded, unassembled, or damaged proteins that could otherwise form potentially toxic aggregates (*1*). Because multiubiquitylated proteins are usually efficiently degraded by cellular proteasomes, the presence of elevated ubiquitin conjugates associated with intracellular deposits of aggregated protein in diseased neurons in nearly all sporadic and hereditary neurodegenerative diseases has long suggested a linkage between UPS dysfunction and pathogenesis (*2*). Recently this linkage has been strengthened by genetic evidence linking mutations in the UPS to several neurodegenerative diseases and models thereof (*3–7*). Despite this evidence, however, the specific causal relation between protein aggregation, UPS activity, and pathogenesis has remained elusive.

To investigate the specific relation between protein aggregation and the function of the UPS, we designed a reporter consisting of a short degron, CL1 (*8*), fused to the COOH-terminus of green fluorescent protein (GFP^u) (*9*). A clonal line of human embryonic kidney (HEK) 293 cells stably expressing GFP^u was isolated and designated GFP^u-1. Pulse-chase analysis (*10*) (Fig. 1A) indicated that GFP^u is

Department of Biological Sciences, Stanford University, Stanford, CA 94305–5020, USA.

*To whom correspondence should be addressed. E-mail: kopito@stanford.edu

unstable [half-time ($t_{1/2}$) = 20 to 30 min] compared with GFP ($t_{1/2}$ > 10 hours). GFP^u was stabilized to the level of GFP when the chase was performed in the presence of the selective proteasome inhibitor lactacystin (*11*). The proteasome inhibitors ALLN and lactacystin, but not other protease inhibitors, increased steady-state GFP^u levels (Fig. 1B) and specific ubiquitylation of GFP^u (Fig. 1C). Thus, the presence of a CL1 degron specifically targeted normally stable GFP for efficient clearance by the UPS.

GFP^u was distributed diffusely in the nuclear and cytoplasmic compartments of GFP^u-1 cells (Fig. 2A), establishing that the CL1 degron did not affect the intracellular trafficking of GFP. The mean fluorescence of GFP^u-1 cells (*12*) increased linearly with time in the presence of proteasome inhibitor, suggesting that GFP^u synthesis is unaffected by proteasome inhibitors (Fig. 2B). GFP^u fluorescence declined rapidly in GFP^u-1 cells after exposure to a protein-synthesis inhibitor (Fig. 2C). The $t_{1/2}$ of GFP^u decline was ~30 min, in good agreement with the pulse-chase $t_{1/2}$ value, and was blocked by the proteasome inhibitor ALLN (Fig. 2C).

To determine whether GFP^u fluorescence is a valid in vivo measure of UPS function, we compared the effect of lactacystin on GFP^u-1 cell fluorescence in vivo with the effect of this inhibitor on proteasome activity (*13*) in cell extracts (Fig. 2D). Whereas 95 nM lactacystin inhibited 50% of chymotrypsin-like activity, a drug concentration of 845 nM was required to produce a 50% maximal increase in GFP^u fluorescence (Fig. 2D). Above 75% inhibition, fluorescence increased steeply with inhibitor concentration (Fig. 2E). Thus, GFP^u fluorescence could be used as a dynamic reporter of UPS activity in vivo, particularly under conditions of substantial UPS inhibition.

To assess the effect of protein aggregation on the UPS, we monitored fluorescence in GFP^u-1 cells transiently expressing aggregation-prone proteins. The ΔF508 mutant of cystic fibrosis membrane conductance regulator (CFTR) quantitatively misfolds in the endoplasmic reticulum (ER) and is exported to the cytoplasm where it is degraded by the UPS (*14*). At low levels of expression, HEK cells are able to suppress ΔF508 aggregation by balancing its synthesis with proteasome-mediated degradation (*15*). In contrast, overexpressed ΔF508 forms stable aggregates that are sequestered by a microtubule-dependent process into pericentriolar cytoplasmic inclusion bodies called aggresomes (*15*). Forty-eight hours after transient transfection of GFP^u-1 cells with a FLAG-ΔF508 expression construct (*16*), 5 to 15% of the FLAG-ΔF508–expressing cells had clearly defined FLAG-immunoreactive aggresomes, whereas the remainder exhibited diffuse, ER localization (Fig. 3A). Cells with FLAG-ΔF508 aggresomes had substantially increased GFP^u fluorescence. To quantify the effect of FLAG-ΔF508 aggregation on GFP^u fluorescence, we analyzed transfected GFP^u-1 cells for FLAG-ΔF508 expression and GFP^u fluorescence by flow cytometry (Fig. 3B). Mean GFP^u fluorescence was 4.26-fold higher in the population of transfected GFP^u-1 cells with high FLAG-ΔF508 expression than in the population of low expressers (Fig. 3B). Moreover, GFP^u fluorescence in individual aggresome-containing cells was, on average, 4.24 times higher than in cells lacking aggre-

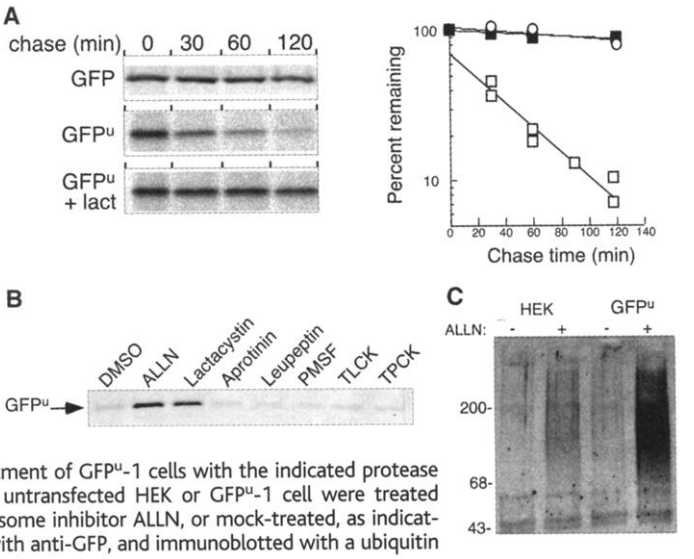

Fig. 1. GFP^u is a substrate of the ubiquitin-proteasome system. (**A**) Pulse-chase analysis of GFP and GFP^u. (Left) Fluorograms of anti-GFP immunoprecipitates sampled at the indicated chase times in the presence or absence of lactacystin. (Right) Quantification of pulse-chase data for GFP^u (squares) and GFP (circles) in the presence (closed symbols) or absence (open symbols) of lactacystin. (**B**) Steady-state level of GFP^u after 5-hour treatment of GFP^u-1 cells with the indicated protease inhibitors. (**C**) Lysates of untransfected HEK or GFP^u-1 cell were treated overnight with the proteasome inhibitor ALLN, or mock-treated, as indicated, immunoprecipitated with anti-GFP, and immunoblotted with a ubiquitin monoclonal antibody.

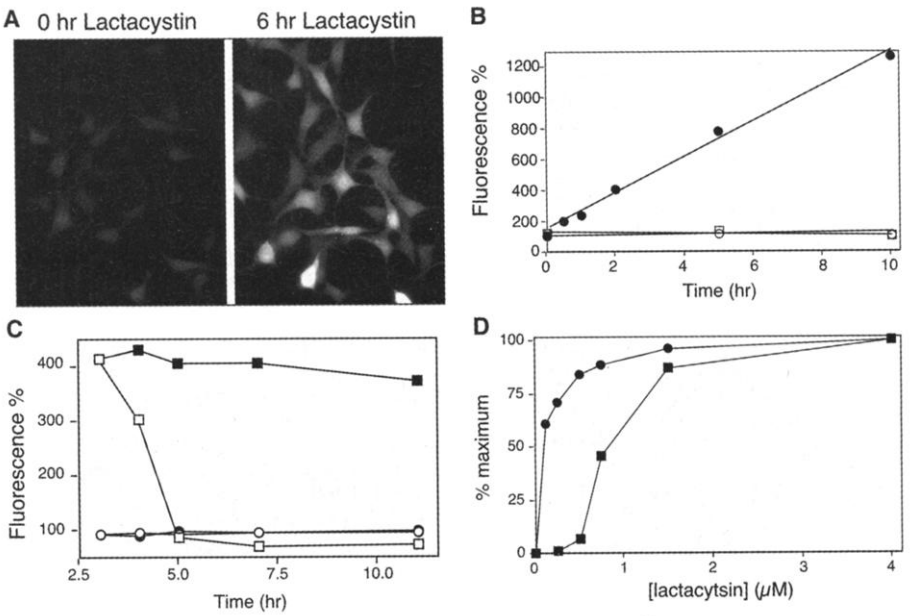

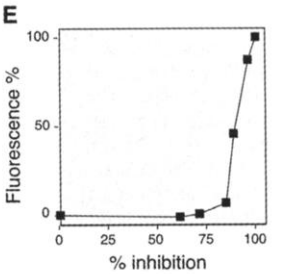

Fig. 2. GFP^u fluorescence is a sensitive measure of UPS activity in vivo. (**A**) GFP^u-1 cells before (left) and after (right) incubation with lactacystin (6 μM). (**B**) Time course of fluorescence in the presence of ALLN (10 μg/ml), assessed by flow cytometry. GFP^u-1 cells (●), HEK cells (○), and GFP-expressing cells (□). (**C**) Degradation kinetics of GFP^u. Fluorescence of GFP^u-1 cells (squares) or stable GFP-expressing cells (circles), assessed by flow cytometry. After a 3-hour incubation with ALLN, cells were incubated with emetine in the presence (closed symbols) or absence (open symbols) of ALLN (10 μg/ml). (**D**) GFP^u fluorescence is a dynamic indicator of UPS activity. GFP^u-1 cells were incubated with lactacystin. Relative GFP^u fluorescence (■), assessed by flow cytometry, and relative inhibition of chymotrypsin-like proteasome activity (●), determined from lysates of lactacystin-treated cells. (**E**) The percentage proteasome inhibition from (D) plotted against GFP^u fluorescence.

somes (Fig. 3C). Thus, the presence of aggregated FLAG-ΔF508 led to inhibition of the UPS.

To assess whether this effect was specific to ΔF508, we tested whether an exon 1 fragment of huntingtin containing an aggregation-promoting expanded polyglutamine homopolymer could inhibit the function of the UPS. Proteins with long poly(Q) (i.e., >35) expansions have an extraordinarily high tendency to aggregate into cytoplasmic and nuclear inclusions in vivo and to form amyloid-like fibrils in vitro (*17*). Poly(Q) aggregation is thought to be mediated by the formation of a network of hydrogen-bonded, β-sheet "polar zippers" (*18*). When expressed in GFP^u-1 cells, Q25-MYC appeared in a bright, but diffuse pattern in the cytoplasmic and nuclear compartments (Fig. 3D). Although most Q103-MYC–expressing cells exhibited similar, diffuse cytoplasmic staining, 10 to 20% had a single prominent juxtanuclear inclusion body that was highly correlated with increased GFP^u fluorescence (Fig. 3, D to F). Mean GFP^u fluorescence of the total population of Q103-MYC–expressing cells with inclusions was 2.3 fold higher ($P < 0.001$) than that of Q25-MYC–transfected cells. Q103-MYC expressers with the largest inclusion bodies exhibited a 4.1-fold higher mean GFP^u fluorescence compared with Q25-MYC transfectants (Fig. 3E). GFP^u fluorescence and inclusion area were positively correlated ($r = 0.661$), further suggesting a linkage between protein aggregation and UPS inhibition (Fig. 3F).

We used ubiquitin immunoblotting to assess the effects of expressing aggregation-prone Q103-GFP huntingtin on accumulation of ubiquitin conjugates (Fig. 4A). HEK cells expressing high levels of Q103-GFP (*19*) exhibited an increased high molecular weight smear of ubiquitin immunoreactivity compared with an identical number of cells expressing low levels of Q103-GFP. This increased level of ubiquitin conjugates could not be explained simply by overexpression of huntingtin, because control cells expressing Q25-GFP and sorted for the same levels of GFP fluorescence exhibited only background levels of ubiquitin conjugates (Fig. 4A).

Cells defective in ubiquitin conjugation (*20*) or exposed to proteasome inhibitor (*21*, *22*) arrest primarily at the G_2/M boundary of the cell cycle. To assess the effect of protein aggregation on the cell cycle, we transfected HEK 293 cells with GFP, Q25-GFP, or Q103-GFP and analyzed the cells by flow cytometry for GFP fluorescence and DNA content (Fig. 4B) (*23*). Cells with the highest level of expression of Q103-GFP had 4*n* DNA content, indicating arrest in G_2. No such subpopulation of cells was observed in cells expressing comparable levels of Q25-GFP or GFP (Fig. 4B).

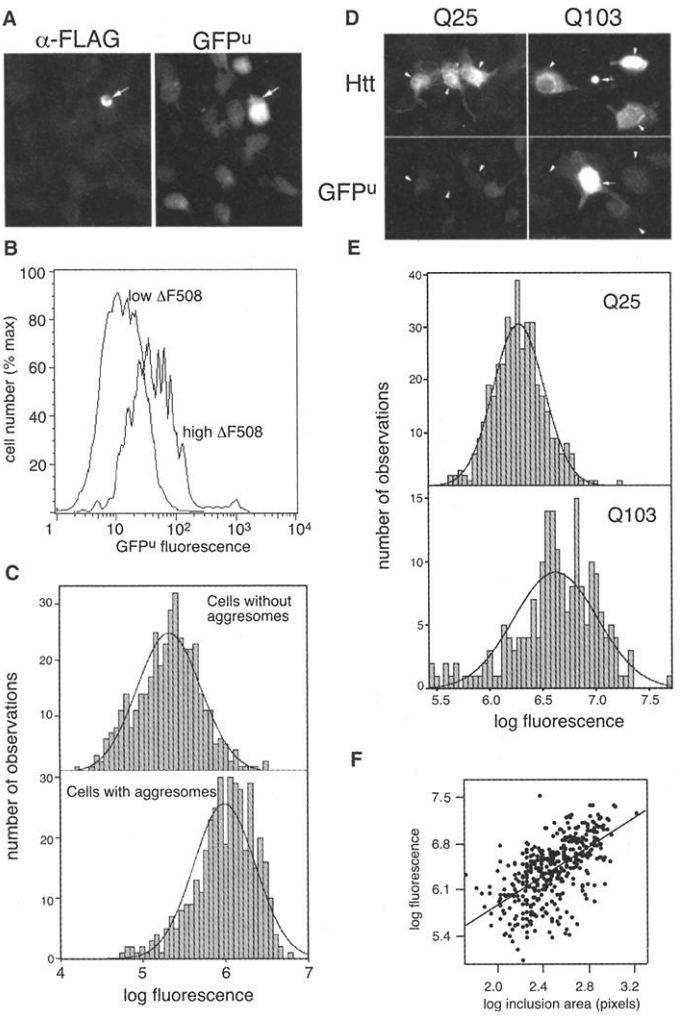

Fig. 3. Protein aggregates inhibit the UPS. (**A**) GFP^u-1 cells transiently transfected with FLAG-ΔF508 imaged for FLAG immunofluorescence or GFP^u fluorescence. The arrow indicates a cell containing a FLAG-ΔF508 aggresome. (**B**). Quantitative analysis of data in (A) showing GFP^u fluorescence (ordinate) in a subpopulation of FLAG-ΔF508–transfected GFP^u-1 cells exhibiting high (top 3%) FLAG-ΔF508 expression compared with GFP^u fluorescence in the subpopulation containing lower (middle 50%) FLAG-ΔF508 expression. (**C**) GFP^u fluorescence, in FLAG-ΔF508–transfected GFP^u-1 cells with (bottom) or without (top) FLAG-immunoreactive aggresomes. (**D**) GFP^u-1 cells transiently transfected with Q25-MYC or Q103-MYC imaged for huntingtin expression (MYC immunocytochemistry) or GFP^u fluorescence (bottom). Inclusion bodies are present in some huntingtin-expressing cells (arrows), but not in others (arrowheads). (**E**) Quantification of data from (D). GFP^u fluorescence in GFP^u-1 cells expressing Q25-MYC (top) or Q103-MYC (bottom) with inclusion bodies larger than 400 pixels. (**F**) Correlation between GFP^u fluorescence and inclusion area in Q103-MYC–transfected GFP^u-1 cells.

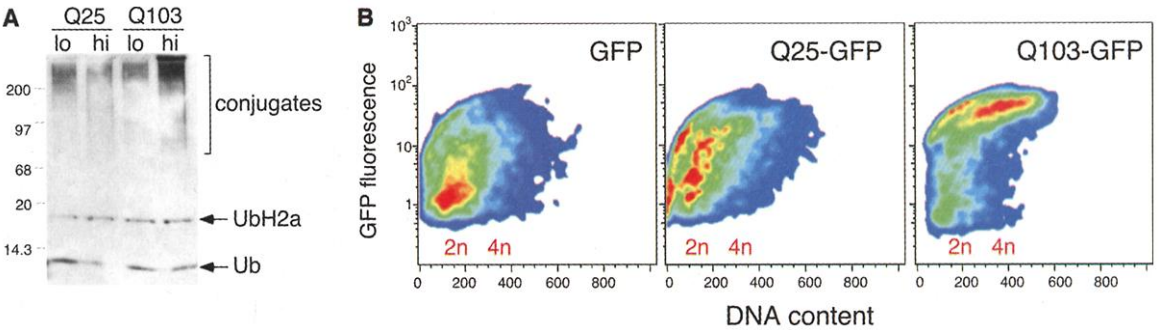

Fig. 4. Protein aggregation induces accumulation of ubiquitin conjugates and cell cycle arrest. (**A**) Ubiquitin immunoblot of lysates of HEK cells transfected with either Q25-GFP or Q103-GFP, as indicated, and sorted into populations containing the lowest or highest 10% of GFP fluorescence. Each lane contains lysates from ~40,000 cells. (**B**) Two-parameter FACS profiles of HEK cells transfected with GFP, Q25-GFP, or Q103-GFP. GFP fluorescence is plotted against DNA content (propidium iodide fluorescence). The fluorescence signals in the two channels are indicated by pseudocolor, with "hot" colors (i.e., red) being highest and "cold" colors (i.e., blue) lowest.

Although it is widely accepted that protein aggregation is a central event in the initiation of cell death in the pathogenesis of inherited neurodegenerative diseases (*24*), the mechanism by which aggregation might be related to a toxic gain-of-function has remained elusive. The above data show that expression of two different, unrelated proteins, sharing only the propensity to misfold and to aggregate, induces substantial increases in intracellular GFP^u fluorescence, indicative of severe disruption of UPS activity. Protein aggregation also leads to accumulation of intracellular ubiquitin conjugates and cell cycle arrest (*25*). These data suggest that protein aggregation causes UPS inhibition.

We find no evidence for decreased free-ubiquitin levels in cells with inclusion bodies (Fig. 4A), suggesting that protein aggregates do not simply deplete pools of intracellular free ubiquitin. Protein aggregates could inhibit the UPS by saturating the capacity of one or more molecular chaperones required for UPS function (*26*) or by direct interaction with the proteasome. Given the processive nature of proteasomal proteolysis (*27*), it is conceivable that proteasomes could become engaged by ubiquitylated aggregates that they can neither unfold nor degrade, and would thus be unavailable for degrading other well-behaved substrates like transcription factors and cyclins. Indeed, proteasome subunits colocalize in inclusion bodies associated with neurodegenerative diseases (*28*, *29*) and experimentally induced aggresomes (*30*, *31*).

Whether protein aggregation is a cause or a consequence of neurotoxicity has been a longstanding conundrum. Our data suggest that resolution of this quandary may lie in the essentially autocatalytic nature of the relation of protein aggregates to the UPS: They are simultaneously inhibitors of the pathway and the products that result from its inhibition. A decline in UPS activity, for any reason, would result in increased production of aggregated proteins and could account for the accumulation of ubiquitin conjugates (*2*) and UPS substrates (*32*) that are aberrantly expressed in diseased neurons. Increased aggregation would lead to a further decline in UPS function. This positive-feedback mechanism might help to explain the often precipitous loss of neuronal function that characterizes the progression of many neurodegenerative diseases.

References and Notes

1. A. Ciechanover, A. Orian, A. L. Schwartz, *Bioessays* **22**, 442 (2000).
2. R. J. Mayer, J. Lowe, G. Lennox, F. Doherty, M. Landon, *Prog. Clin. Biol. Res.* **317**, 809 (1989).
3. C. J. Cummings *et al.*, *Neuron* **24**, 879 (1999).
4. P. Fernandez-Funez *et al.*, *Nature* **408**, 101 (2000).
5. T. Kitada *et al.*, *Nature* **392**, 605. (1998).
6. K. Saigoh *et al.*, *Nature Genet.* **23**, 47 (1999).
7. E. Leroy *et al.*, *Nature* **395**, 451 (1998).
8. T. Gilon, O. Chomsky, R. G. Kulka, *EMBO J.* **17**, 2759 (1998).
9. The GFP^u plasmid was created by ligating an oligonucleotide encoding ACKNWFSSLSHFVIHL into the GFP-C1 plasmid (Clontech).
10. Cells were labeled with ^{35}S-Met and ^{35}S-Cys for 10 min, chased, and lysed by sonication in phosphate-buffered saline containing 1% Triton X-100. Lysates were immunoprecipitated with antibody to GFP (anti-GFP) and resolved by SDS–polyacrylamide gel electrophoresis (SDS-PAGE). For immunoblotting, cells were lysed in 10 mM tris (pH 7.4), 5 mM EDTA with 1% Triton X-100.
11. Clasto-lactacystin β-lactone, the active form of lactacystin, was used in this study.
12. For GFP^u-1 characterization, 10,000 to 15,000 cells were analyzed on a flow cytometer.
13. The chymotrypsin-like peptidase activity of the proteasome was assayed with the fluorogenic substrate, succinyl-Leu-Leu-Val-Tyr-AMC. Cells were treated with the irreversble inhibitor lactacystin, washed, lysed in buffer containing 10 mM tris (pH 7.5), 1 mM EDTA, 20% glycerol, 2 mM adenosine 5′-triphosphate, 0.5% Triton X-100, and protease inhibitors [50 μM phenylmethylsulfonyl fluoride, 50 μM TPCK (tosyl phenylalanyl chloromethylketone), 2 μg/ml aprotinin, and 2 μg/ml leupeptin] and incubated with 1 mM substrate at room temperature for 3 hours.
14. R. R. Kopito, *Physiol. Rev.* **79**, S167 (1999).
15. J. A. Johnston, C. L. Ward, R. R. Kopito, *J. Cell Biol.* **143**, 1883 (1998).
16. The FLAG-ΔF508 construct was generated from FLAG-CFTR (*33*).
17. H. Y. Zoghbi, H. T. Orr, *Annu. Rev. Neurosci.* **23**, 217 (2000).
18. M. F. Perutz, T. Johnson, M. Suzuki, J. T. Finch, *Proc. Natl. Acad. Sci. U.S.A.* **91**, 5355 (1994).
19. For analysis of ubiquitin conjugates, ~200,000 cells, collected by fluorescence-activated cell sorting (FACS) from the top 10% and lowest 10% of cells expressing Q25-GFP and Q103-GFP, were lysed in SDS sample buffer and resolved by SDS-PAGE.
20. D. Finley, A. Ciechanover, A. Varshavsky, *Cell* **37**, 43 (1984).
21. S. W. Sherwood, A. L. Kung, J. Roitelman, R. D. Simoni, R. T. Schimke, *Proc. Natl. Acad. Sci. U.S.A.* **90**, 3353 (1993).
22. C. Wojcik, D. Schroeter, M. Stoehr, S. Wilk, N. Paweletz, *Eur. J. Cell Biol.* **70**, 172 (1996).
23. For cell cycle analyses, HEK 293 cells were fixed in 4% paraformaldehyde 72 hours after transfection and treated with 5 μg/ml ribonuclease A for 2 hours at room temperature, stained with 10 μg/ml propidium iodide, and analyzed for DNA and GFP content by flow cytometry.
24. J. B. Schulz, J. Dichgans, *Curr. Opin. Neurol.* **12**, 433 (1999).
25. Overexpression of GFP^u, itself a short-lived protein, does not cause cell cycle arrest, indicating that the observed increase is not due simply to the presence of an abundant UPS substrate.
26. B. Bercovich *et al.*, *J. Biol. Chem.* **272**, 9002 (1997).
27. T. N. Akopian, A. F. Kisselev, A. L. Goldberg, *J. Biol. Chem.* **272**, 1791 (1997).
28. S. Kwak, T. Masaki, S. Ishiura, H. Sugita, *Neurosci. Lett.* **128**, 21 (1991).
29. C. J. Cummings *et al.*, *Nature Genet.* **19**, 148 (1998).
30. W. C. Wigley *et al.*, *J. Cell Biol.* **145**, 481 (1999).
31. R. Garcia-Mata, Z. Bebok, E. J. Sorscher, E. S. Sztul, *J. Cell Biol.* **146**, 1239 (1999).
32. A. K. Raina, X. Zhu, M. Monteiro, A. Takeda, M. A. Smith, *Prog. Cell Cycle Res.* **4**, 235 (2000).
33. M. Howard *et al.*, *Am. J. Physiol.* **269**, C1565 (1995).

34. We thank R. Frizzell for FLAG-CFTR, A. Tobin for huntingtin plasmids, M. Bucci for the GFP cell line, M. Rexach for anti-GFP, and C. Carswell-Crumpton for assistance with flow cytometry. We also thank R. Rajan and other members of the Kopito laboratory for stimulating discussions. Supported in part by a research grant from the National Institutes of Health, a Howard Hughes Summer Fellowship from the Department of Biological Sciences at Stanford University, and an NIH predoctoral training grant.

6 February 2001; accepted 19 April 2001